

Building Alkali-Metal-Halide Layers within a Perovskite Host by Sequential Intercalation: $(A_2Cl)LaNb_2O_7$ (A = Rb, Cs)

Jonglak Choi, Xiao Zhang, and John B. Wiley*

Department of Chemistry and the Advanced Materials Research Institute, University of New Orleans, New Orleans, Louisiana 70148

Received December 8, 2008

Alkali-metal-halide layers were constructed within Dion–Jacobson (DJ) layered perovskites by a two-step sequential intercalation method. Reductive intercalation with an alkali metal, followed by oxidative intercalation with chlorine gas, leads to the formation of the compounds, $(A_2Cl)LaNb_2O_7$ (A = Rb, Cs). Rietveld refinement of X-ray powder diffraction data shows that an alkali-metal-halide layer is formed between the perovskite blocks. The alkali-metal cation is eight-coordinate with four oxygens from the perovskite layer and four chlorides from the new halide layer; this environment is similar to cesium in the CsCl structure (B2). Thermal analysis indicates that these are low-temperature phases where decomposition begins by 400 °C. Details on the synthesis and characterization of this set of compounds are presented, and the general utility of this approach discussed.

Introduction

Topochemical reactions, such as ion exchange and intercalation/deintercalation, are powerful tools for carrying out structural modifications on receptive host compounds at low temperatures. Strategies based on these methods can be effective in forming new materials with interesting new structural, magnetic, and electronic properties.^{1–6} One continuing goal in this work is to develop an extensive reaction library that can serve in the directed (premeditated) construction of new active structural features. This ability could allow researchers to more effectively design new technologically significant materials such as high temperature superconductors, magnetoresistive materials, and ferroelectrics.

Recently researchers have been quite successful in the manipulation of a variety of perovskite systems by topo-

chemical methods.^{7–9} Reactions with the layered perovskites Dion–Jacobson (DJ), $A[A'_{n-1}B_nO_{3n+1}]$, and Ruddlesden–Popper (RP), $A_2[A'_{n-1}B_nO_{3n+1}]$ (A is an alkali-metal cation, A' is typically an alkaline-earth or rare-earth cation, and B a d⁰ transition metal cation), have been especially fruitful. These sets of compounds readily undergo ion exchange^{10–13} and the DJ series are also receptive to reductive intercalation.^{14–16} One goal among current researchers has been to use such layered hosts as templates for the interlayer growth of new metal-anion arrays; the formation of such layers can be viewed analogously to epitaxial thin film growth, though here the new layer forms within a crystal instead of on the surface. Some of the initial reports in this area have involved the formation of transition-metal-halide and metal-oxide layers. Metal-halide layers (MX; M = V, Cr, Mn, Fe, Co, Cu; X = Cl (and Br for M = Cu)) have been constructed within DJ hosts by ion exchange with simple metal halides

*To whom correspondence should be addressed. E-mail: jwiley@uno.edu.

- (1) Schaak, R. E.; Mallouk, T. E. *Chem. Mater.* **2002**, *14*, 1455.
- (2) Gopalakrishnan, J. *Chem. Mater.* **1995**, *7*, 1265.
- (3) Tsujimoto, Y.; Tassel, C.; Hayashi, N.; Watanabe, T.; Kageyama, H.; Yoshimura, K.; Takano, M.; Ceretti, M.; Ritter, C.; Paulus, W. *Nature (London)* **2007**, *45*, 7172.
- (4) Yoshida, M.; Ogata, N.; Takigawa, M.; Yamaura, J.; Ichihara, M.; Kitano, T.; Kageyama, H.; Ajiro, Y.; Yoshimura, K. *J. Phys. Soc. Jpn.* **2007**, *76*, 104703.
- (5) Kageyama, H.; Watanabe, T.; Tsujimoto, Y.; Kitada, A.; Sumida, Y.; Kanamori, K.; Yoshimura, K.; Hayashi, N.; Muranaka, S.; Takano, M.; Ceretti, M.; Paulus, W.; Ritter, C.; Andre, G. *Angew. Chem., Int. Ed.* **2008**, *47*, 5740.
- (6) Machida, M.; Yabunaka, J. i.; Kijima, T. *Chem. Mater.* **2000**, *12*, 812.
- (7) Caignaert, V.; Millange, F.; Domenges, B.; Raveau, B.; Suard, E. *Chem. Mater.* **1999**, *11*(4), 930.

- (8) Gönen, Z. S.; Paluchowski, D.; Zavalij, P.; Eichhorn, B. W.; Gopalakrishnan, J. *Inorg. Chem.* **2006**, *45*, 8736.
- (9) Schottenfeld, J. A.; Kobayashi, Y.; Wang, J.; Macdonald, D. D.; Mallouk, T. E. *Chem. Mater.* **2008**, *20*, 213.
- (10) Gopalakrishnan, J.; Bhat, V.; Raveau, B. *Mater. Res. Bull.* **1987**, *22*, 413.
- (11) Sato, M.; Abo, J.; Jin, T.; Ohta, M. *J. Alloys Comp.* **1993**, *192*, 81.
- (12) Sato, M.; Abo, J.; Jin, T. *Solid State Ionics* **1992**, *57*, 285.
- (13) Sato, M.; Jin, T.; Ueda, H. *Chem. Lett.* **1994**, *1*, 161.
- (14) Armstrong, A. R.; Anderson, P. A. *Inorg. Chem.* **1994**, *33*, 4366.
- (15) Toda, K.; Takahashi, M.; Teranishi, T.; Ye, Z. G.; Sato, M.; Hinatsu, Y. *J. Mater. Chem.* **1999**, *9*, 799.
- (16) Bohnke, C.; Bohnke, O.; Fourquet, J. L. *J. Electrochem. Soc.* **1997**, *144*, 1151.

(MX₂) to produce compounds such as (MX)LaNb₂O₇.^{17–22} Metal-oxide layers have been inserted into layered perovskites by reactions with mixed-metal oxyhalides;^{23,24} Ca₂La₂CuTi₂O₁₀, for example, has been prepared from NaLaTiO₄ and Ca₂CuO₂Cl₂.²⁴ Multistep topochemical reaction strategies have also been reported. Methods involving a combination of ion exchange and reductive intercalation were utilized to construct tetrahedrally coordinated lithium- and sodium-chloride layers within DJ hosts.^{25,26} Herein we report a new multistep reaction strategy for the fabrication of metal-halide arrays with large alkali-metal cations. A two-step sequential reductive-oxidative intercalation procedure is used to build alkali-metal-halide layers within a layered perovskite. The resulting new compounds, (A₂Cl)LaNb₂O₇ (A = Rb, Cs), have alkali-halide layers with cesium-chloride-like structural features.²⁷

Experimental Section

Synthesis. ALaNb₂O₇ (A = Li, Na, K, Rb, and Cs). RbLaNb₂O₇ and CsLaNb₂O₇ were prepared by methods similar to those reported in the literature;^{10,28,29} well-ground stoichiometric mixtures of La₂O₃ (Alfa Aesar, 99.99%), Nb₂O₅ (Alfa Aesar, 99.9985%), and a 25% molar excess of Rb₂CO₃ (Alfa Aesar, 99.0%) or Cs₂CO₃ (Alfa Aesar, 99.9%), respectively, were heated for ~12 h at 850 °C and for 24 h at 1050 °C with one intermediate grinding. The excess of carbonate was added to balance that lost because of volatilization. After the reaction, the products were washed thoroughly with distilled water and dried with acetone followed by overnight heating at 150 °C. The other members of the series, ALaNb₂O₇ (A = Li, Na, and K), were obtained by ion exchange of RbLaNb₂O₇ with a 10:1 molar ratio of the alkali metal nitrates, LiNO₃ (Alfa Aesar, 99.0% anhydrous), NaNO₃ (Alfa Aesar, 99.999%), and KNO₃ (Alfa Aesar, 99.997%), for 4 days at 300, 310, and 350 °C, respectively.^{10–12} The resulting products, LiLaNb₂O₇ and KLaNb₂O₇, were washed with distilled water and dried with acetone followed by overnight heating at 150 °C. After washing, the hygroscopic NaLaNb₂O₇ was dried at 260 °C in air¹⁸ and quickly transferred to a drybox. The unit cells of the products, as determined by X-ray powder diffraction, were all in good agreement with published results.^{10–14}

Reductive Intercalation. A₂LaNb₂O₇ (A = Li, Na, K, Rb, and Cs) were prepared by reductive intercalation of the ALaNb₂O₇ series. Initially ALaNb₂O₇ pellets (typically 0.5 g, 7 mm dia.), prepared with a simple hand press (Aldrich Quick Press), were placed in a Pyrex tube, and thoroughly dried with a heat gun under dynamic vacuum. Cs₂LaNb₂O₇ was obtained by intercalation of CsLaNb₂O₇ with Cs metal vapor (Alfa Aesar, 99.98%). A slight excess of alkali metal, molar ratio of about 1: < 1.05, was weighed out onto a small piece of Pyrex tubing (6 mm dia., closed one end) for ease of handling. (The excess Cs partially compensated for the minimal surface oxidation that occurred during sample preparation.) The alkali metal and 0.5 g of CsLaNb₂O₇ pellets were placed in a Pyrex tube (12 mm dia.) and then sealed under vacuum (< 10⁻⁴ torr). No direct contact occurred between the alkali metal and the pellets before heating. The Pyrex tube was heated for 4 days at 290 °C in a tube furnace. During the reaction, pellets tended to fracture into smaller pieces, likely because of the volume expansion that occurred on reaction. The tube was periodically rotated to expose fresh sample surfaces to the alkali metal vapor. The product Cs₂LaNb₂O₇ showed a homogeneous blue-black color. To distill away any unreacted alkali metal from the product, the sample tube was heated in a temperature gradient (200 °C → RT) for 7 days.

The Na (Alfa Aesar, 99.95%), K (Alfa Aesar, 99.95%), and Rb (Alfa Aesar, 99.75%) analogues were prepared by a similar procedure,¹⁴ except that samples were heated at 310, 290, and 250 °C, respectively. In the case of Na, a significant amount of the metal reacted with the Pyrex tube; therefore, a larger excess of the metal, 1:1.3 molar ratio, was necessary. Lithium intercalation to form Li₂LaNb₂O₇ from LiLaNb₂O₇ was performed with an excess of *n*-BuLi (Aldrich, 2.5 M in hexane), 1:10 molar ratio.¹³ The reaction was carried out with constant stirring at ambient temperature on a Schlenk line under argon atmosphere for 4 days. Before drying, the product was washed several times with dry hexane until no lithium residue was found in the filtrate solution.

The A₂LaNb₂O₇ intercalation products are especially air sensitive; their reactivity to air (presumably moisture) increases as one moves down the periodic table with rubidium and cesium compounds showing an almost instantaneous response on exposure. Cs₂LaNb₂O₇ for example immediately turns from dark blue-black to white with X-ray powder diffraction showing a conversion (deintercalation) back to CsLaNb₂O₇. Therefore, all intercalation reagents and products were handled in an argon-filled drybox to minimize exposure to water and oxygen. **Caution!** Elemental alkali-metal reagents can explosively react with water, and should be handled and disposed with extreme care.

Oxidative Intercalation. The reductive intercalation products, A₂LaNb₂O₇, were reacted with chlorine gas (Matheson, 99.99%). A Schlenk line, interfaced to a sulfuric acid scrubber similar to that described by Jolly,³⁰ was used for the chlorine reactions. To remove excess chlorine, gases exited through a saturated aqueous KOH solution. The entire system was maintained in a well-ventilated fume hood. In the case of Cs₂LaNb₂O₇, about 0.3 g of compound was loaded under argon into a 20 mL scintillation vial fitted with a TFE/silicone septa cap. The reaction vial was connected to the Schlenk line by two stainless steel cannulas and purged with nitrogen for about 30 min before the introduction of chlorine gas (ca. 10 cc/min). The initially blue-black color of the Cs₂LaNb₂O₇ sample changed to white after a few minutes of chlorine exposure at room temperature. The reaction was exothermic as indicated by the noticeable increase in the temperature of the sample vial. After an hour exposure to flowing Cl₂, the system was then flushed for a few hours with nitrogen to purge any unreacted chlorine gas. The other analogues were treated in a similar fashion except the

(17) Kodenkandath, T. A.; Lalena, J. N.; Zhou, W. L.; Carpenter, E. E.; Sangregorio, C.; Falster, A. U.; Simmons, W. B. Jr.; O'Connor, C. J.; Wiley, J. B. *J. Am. Chem. Soc.* **1999**, *121*, 10743.

(18) Kodenkandath, T. A.; Kumbhar, A. S.; Zhou, W. L.; Wiley, J. B. *Inorg. Chem.* **2001**, *40*, 710.

(19) Viciu, L.; Caruntu, G.; Royant, N.; Koenig, J.; Zhou, W. L.; Kodenkandath, T. A.; Wiley, J. B. *Inorg. Chem.* **2002**, *41*, 3385.

(20) Viciu, L.; Koenig, J.; Spinu, L.; Zhou, W. L.; Wiley, J. B. *Chem. Mater.* **2003**, *15*, 1480.

(21) Tsujimoto, Y.; Kageyama, H.; Baba, Y.; Kitada, A.; Yamamoto, T.; Narumi, Y.; Kindo, K.; Nishi, M.; Carlo, J. P.; Aczel, A. A.; Williams, T. J.; Goko, T.; Luke, G. M.; Uemura, Y. J.; Ueda, Y.; Ajiro, Y.; Yoshimura, K. *Phys. Rev. B* **2008**, *78*, 214410.

(22) Tsujimoto, Y.; Baba, Y.; Oba, N.; Kageyama, H.; Fukui, T.; Narumi, Y.; Kindo, K.; Saito, T.; Takano, M.; Ajiro, Y.; Yoshimura, K. *J. Phys. Soc. Japan* **2007**, *76*, 063711.

(23) Gopalakrishnan, J.; Sivakumar, T.; Ramesha, K.; Thangadurai, V.; Subbanna, G. N. *J. Am. Chem. Soc.* **2000**, *122*, 6237.

(24) Sivakumar, T.; Lofland, S. E.; Ramanujachary, K. V.; Ramesha, K.; Subbanna, G. N.; Gopalakrishnan, J. *J. Solid State Chem.* **2004**, *177*, 2635.

(25) Viciu, L.; Kodenkandath, T. A.; Wiley, J. B. *J. Solid State Chem.* **2007**, *180*, 583.

(26) Viciu, L.; Zhang, X.; Kodenkandath, T. A.; Golub, V.; Wiley, J. B. *Mater. Res. Soc. Symp. Proc.* **2007**, *988*, 0988-QQ08-04.

(27) It should be noted that preliminary results for (Rb₂Cl)LaNb₂O₇ were initially revealed in reference 26.

(28) Dion, M.; Ganne, M.; Tournoux, M. *Mater. Res. Bull.* **1981**, *16*, 1429.

(29) Viciu, L.; Lizard, N.; Golub, V.; Kodenkandath, T. A.; Wiley, J. B. *Mater. Res. Bull.* **2007**, *42* (1), 196.

(30) Jolly, W. L. *The Synthesis and Characterization of Inorganic Compounds*; Prentice-Hall Inc.: NJ, 1970.

exposure time to the chlorine gas varied because of the differences in reactivity: $\text{Rb}_2\text{LaNb}_2\text{O}_7$ was treated for an hour, and $\text{A}_2\text{LaNb}_2\text{O}_7$ ($\text{A} = \text{Li, Na, and K}$) for up to 4 h. In addition, $\text{Na}_2\text{LaNb}_2\text{O}_7$ and $\text{K}_2\text{LaNb}_2\text{O}_7$, were treated at elevated temperatures (ca. $> 100^\circ\text{C}$) in the flowing chlorine gas. **Caution!** Chlorine is a highly corrosive and toxic gas that should be handled with extreme caution.

Both the rubidium and cesium samples readily underwent oxidative intercalation with chlorine to produce $(\text{A}_2\text{Cl})\text{LaNb}_2\text{O}_7$ plus trace amounts of ACl . These reactions are exothermic; though there was no obvious effect with the rubidium sample, providing a heat sink (room temperature water bath) for the cesium compound noticeably reduced the amount of CsCl in the product. Alternative efforts to remove the ACl impurities were unsuccessful; while neither of these products showed obvious moisture sensitivity on air exposure of several weeks, they were water sensitive in that a simple water wash resulted in deintercalation back to the ALaNb_2O_7 ($\text{A} = \text{Rb, Cs}$) starting compounds.

On chlorine treatment, the other compounds showed distinctly different behaviors. The lithium sample quickly deintercalated to produce $\text{LiLaNb}_2\text{O}_7$ and LiCl , and the sodium compound was relatively inert showing only trace amounts of NaCl , even with heating. The potassium sample deintercalated very slowly, even with heating, to produce KLaNb_2O_7 and KCl , though in some instances, a broad low angle reflection at $\sim 6.6^\circ 2\theta$ was observed, possibly indicating chlorine intercalation.

Characterization. X-ray powder diffraction data were collected on a Philips X'Pert system equipped with a curved graphite monochromator and $\text{Cu K}\alpha$ radiation ($\lambda = 1.5418\text{\AA}$). Standard scans were collected in continuous mode from 5 to $75^\circ 2\theta$ with a scan rate of 0.01 deg/s . Air-sensitive samples of $\text{A}_2\text{LaNb}_2\text{O}_7$ ($\text{A} = \text{Li, Na, K, Rb, and Cs}$) compounds were sealed under polypropylene film with silicon grease prior to data collection. Peak positions were determined with the program PROFILE FIT.³¹ Lattice parameters were refined by a least-squares method with the program POLSQ.³² The crystal structures of $(\text{A}_2\text{Cl})\text{LaNb}_2\text{O}_7$ ($\text{A} = \text{Rb, Cs}$) were refined by the Rietveld method with FullProf.³³ Data used for Rietveld refinement were collected as step scans with 0.02° steps and 10 s count times from 10 to $90^\circ 2\theta$. A total of 30 parameters were refined including scale factor, zero-point shift, six background parameters, cell constants, atomic coordinates, peak shape, thermal parameters, and absorption coefficients. The Thompson–Cox–Hastings pseudo-Voigt function was used in the profile refinement. The R factor (R_p), the weighted R factor (R_{wp}), and χ^2 are defined as the following: profile, $R_p = 100[\sum |y_{oi} - y_{ci}| / \sum |y_{oi}|]$; weighted profile, $R_{wp} = 100[\sum w_i |y_{oi} - y_{ci}|^2 / \sum w_i |y_{oi}|^2]^{1/2}$; and goodness of fit (GOF), $\chi^2 = [R_{wp}/R_{exp}]^2$ where $R_{exp} = 100 [(N - P) / \sum w_i |y_{oi}|^2]^{1/2}$, y_{oi} and y_{ci} are the observed and calculated intensities, w_i is the weighting factor, N is the total number of y_{oi} data when the background is refined, P is the number of adjusted parameters.

Elemental analysis was carried out by energy dispersive spectroscopy (EDS) on a JEOL JSM 5410 scanning electron microscope equipped with an EDAX-DX Prime microanalytical system. For $(\text{Cs}_2\text{Cl})\text{LaNb}_2\text{O}_7$, the molar ratios between elements are comparable to the ideal ratio, as Cs [1.831(8)]: Cl [0.918(9)]: La [1.00]: Nb [1.87(1)], where the ratio was normalized to lanthanum. In the case of $(\text{Rb}_2\text{Cl})\text{LaNb}_2\text{O}_7$, a number of L-lines and K-lines for rubidium and niobium overlapped making resolution of these data difficult; the ratio of chlorine to lanthanum, however, was consistently 1:1.

Both high temperature XRD (HTXRD) and differential scanning calorimetry (DSC) were performed. High temperature XRD experiments were carried out to over 700°C on the Philips X-Pert system equipped with an Anton Paar high temperature stage. DSC measurements were executed on a Netzsch 404S thermal analysis system in flowing argon in alumina pans; samples were heated to 1000°C at a rate of 5°C/min .

Results

Oxidative intercalation of $\text{A}_2\text{LaNb}_2\text{O}_7$ with chlorine gas readily occurs at room temperature for the rubidium and cesium compounds. Similar reactions with other alkali-metal analogues were not successful; in the case of $\text{Li}_2\text{LaNb}_2\text{O}_7$, deintercalation of lithium rapidly occurred to form LiCl and the parent compound, $\text{LiLaNb}_2\text{O}_7$, and for the sodium and potassium systems, these compounds were relatively inert. Some indication for the possible formation of poorly crystalline $(\text{K}_2\text{Cl})\text{LaNb}_2\text{O}_7$ was observed, but efforts to tune the reaction conditions for this compound were unsuccessful.

Figure 1 shows the variation in the X-ray powder diffraction patterns in going from $\text{CsLaNb}_2\text{O}_7$ to $\text{Cs}_2\text{LaNb}_2\text{O}_7$, and then to $(\text{Cs}_2\text{Cl})\text{LaNb}_2\text{O}_7$. A very small amount of CsCl is also formed in the chlorine reaction as indicated by an asterisk. The $(\text{A}_2\text{Cl})\text{LaNb}_2\text{O}_7$ ($\text{A} = \text{Rb, Cs}$) final products are readily indexed on tetragonal unit cells. Table 1 compares the unit cells for the reaction series of both the rubidium and cesium, where parameters of precursor phases were determined by least-squares method. While there is only a slight increase in the layer spacing of the perovskite host on intercalation of rubidium (0.15 \AA) or cesium (0.50 \AA), on intercalation of chlorine, the increase relative to the parent is much greater, 3.91 \AA and 4.14 \AA for the rubidium and cesium compounds, respectively.

Rietveld refinement was carried out on $(\text{Cs}_2\text{Cl})\text{LaNb}_2\text{O}_7$. The starting model was based on the simple insertion of a CsCl layer (B_2 structure type, cubic coordination for both cations and anions) into the parent compound, $\text{CsLaNb}_2\text{O}_7$, with the space group $P4/mmm$. The observed, calculated, and difference plots for the refinement are shown in Figure 2. Regions containing reflections of the minor CsCl impurity were excluded. The crystallographic data for $(\text{Cs}_2\text{Cl})\text{LaNb}_2\text{O}_7$ are presented in Table 2. Occupation factors (g) were refined

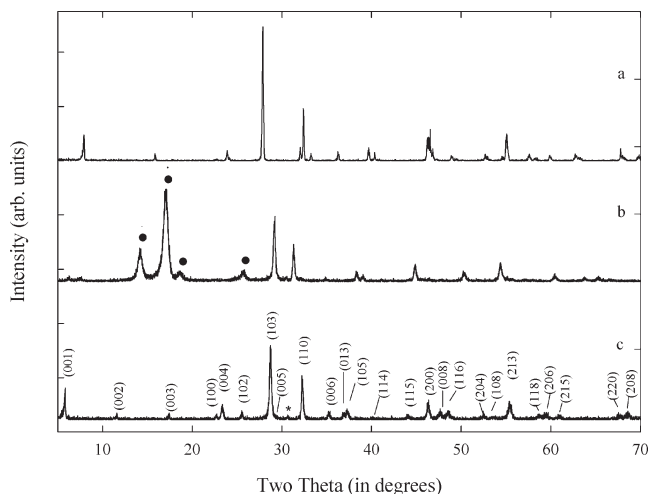


Figure 1. X-ray powder diffraction patterns for (a) $\text{CsLaNb}_2\text{O}_7$; (b) $\text{Cs}_2\text{LaNb}_2\text{O}_7$; (c) $(\text{Cs}_2\text{Cl})\text{LaNb}_2\text{O}_7$. The highly air-sensitive $\text{Cs}_2\text{LaNb}_2\text{O}_7$ was covered with polypropylene film; peaks from this film are marked (●). The trace impurity of CsCl in the final product is indicated by an asterisk (*).

(31) Sconneveld, E. J.; Delhez, R. *ProFit 1.0C*; 1996.

(32) Keszler, A. D.; Ibers, J. A. *Modified POLSQ*; Department of Chemistry, Northwestern University: Evanston, IL, 1983.

(33) R-Carvajal, J. *Recent Developments of the Program FULLPROF, in Commission on Powder Diffraction (IUCr)* **2001**, 26, 12.

Table 1. Crystal Systems, Unit Cell Parameters, Volumes, and Spacings between Perovskite Layers for the Reaction Series $A\text{LaNb}_2\text{O}_7$, $A_2\text{LaNb}_2\text{O}_7$, and $(A_2\text{Cl})\text{LaNb}_2\text{O}_7$ ($A = \text{Rb}, \text{Cs}$)

compound	crystal system (space group)	unit cell parameters (Å) (volume Å ³)	literature values (Å) (volume Å ³)	layer spacing (Å)	literature reference
$\text{RbLaNb}_2\text{O}_7^a$	orthorhombic (<i>Imma</i>)	$a = 5.497(3)$ $b = 21.99(1)$ $c = 5.506(6)$ (665.56(1) Å ³)	$a = 5.4941(1)$ $b = 21.9901(6)$ $c = 5.4925(4)$ (663.58 Å ³)	11.00	14
$\text{Rb}_2\text{LaNb}_2\text{O}_7^a$	orthorhombic (<i>Cmcm</i>)	$a = 22.29(3)$ $b = 5.704(4)$ $c = 5.67(1)$ (720.89(2) Å ³)	$a = 22.30955(9)$ $b = 5.69748(10)$ $c = 5.69365(10)$ (723.71 Å ³)	11.15	14
$(\text{Rb}_2\text{Cl})\text{LaNb}_2\text{O}_7^b$	tetragonal (<i>P4/mmm</i>)	$a = 3.887(1)$ $c = 14.913(1)$ (225.32(1) Å ³)		14.91	this work
$\text{CsLaNb}_2\text{O}_7^a$	tetragonal (<i>P4/mmm</i>)	$a = 3.906(1)$ $c = 11.17(1)$ (170.42(1) Å ³)	$a = 3.908(1)$ $c = 11.160(4)$ (170.4 Å ³)	11.17	34
$\text{Cs}_2\text{LaNb}_2\text{O}_7^a$	orthorhombic (<i>Cmcm</i>)	$a = 23.33(1)$ $b = 5.871(6)$ $c = 5.619(5)$ (769.63(3) Å ³)		11.67	this work
$(\text{Cs}_2\text{Cl})\text{LaNb}_2\text{O}_7^b$	tetragonal (<i>P4/mmm</i>)	$a = 3.92182(1)$ $c = 15.3107(3)$ (235.489(6) Å ³)		15.31	this work

^a Lattice parameters refined with POLSQ. ^b Values from Rietveld refinement.

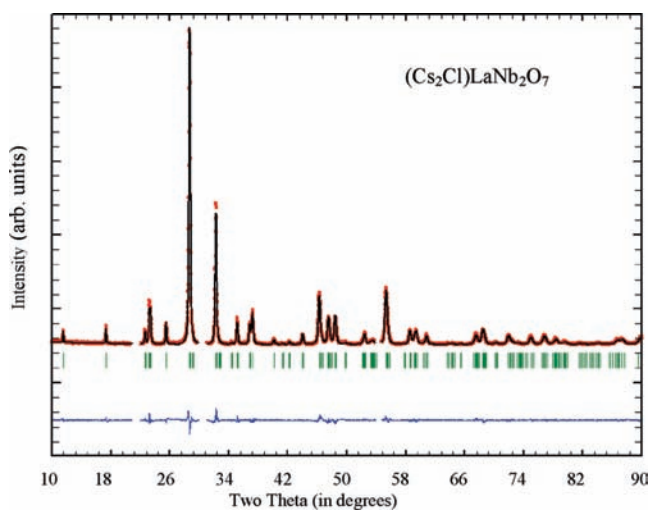


Figure 2. Observed and calculated data for the Rietveld refinement of $(\text{Cs}_2\text{Cl})\text{LaNb}_2\text{O}_7$. Observed data are indicated by crosses, calculated pattern by a solid line, reflections are indicated immediately below diffraction data by tick marks, and the bottom curve is the difference plot. The excluded regions correspond to the CsCl minor impurity.

Table 2. Crystallographic Data for $(\text{Cs}_2\text{Cl})\text{LaNb}_2\text{O}_7$ at Room Temperature^a

atoms	site	x	y	z	$B_{\text{iso}}(\text{Å}^2)$	g
Cs	2g	0	0	0.3609(1)	1.5(1)	0.96(1)
Cl	1d	1/2	1/2	1/2	1.3(3)	0.97(2)
La	1a	0	0	0	1.09(1)	1
Nb	2h	1/2	1/2	0.1460(2)	0.4(1)	1
O1	2h	1/2	1/2	0.2564(9)	2.7(5)	1
O2	1c	1/2	1/2	0	2.0 ^b	1
O3	4i	0	1/2	0.1231(6)	2.9(3)	1

^a *P4/mmm*; $Z = 1$; $R_p = 7.91\%$, $R_{wp} = 11.1\%$, and $\chi^2 = 2.06\%$. ^b Oxygen (O2) parameter fixed at 2.0.

for cesium and chloride and indicated almost full occupation of these sites. During the refinement, the thermal parameter of niobium was found to be unstable, tending to go negative. Inclusion of an absorption correction removed this

Table 3. Selected Bond Distances for $(\text{Cs}_2\text{Cl})\text{LaNb}_2\text{O}_7$

bond types	length (Å)
Cs–Cl × 4	3.497(1)
Cs–O1 4	3.199(7)
Nb–O1 × 1	1.70(1)
Nb–O2 × 1	2.233(3)
Nb–O3 × 4	1.993(2)
La–O2 × 4	2.7731(1)
La–O3 × 8	2.7160(6)

instability. After the correction, however, the thermal parameter for oxygen O2 (O2 links niobiums along c-direction) became unreasonably large. Efforts to disorder O2 onto lower symmetry positions, from (0.5, 0.5, 0) to (x, 0.5, 0), (x, 0.5, z), (x, x, 0), and (x, x, z), did not result in improvement in the fit nor did it give a model that made structural sense in terms of possible tilting mechanisms for NbO_6 octahedra. Consequently, the oxygen thermal parameter was fixed at 2.0 (see Tables 2 and 3).

The final structure for $(\text{Cs}_2\text{Cl})\text{LaNb}_2\text{O}_7$ is shown in Figure 3. The perovskite layers of the host compound are maintained in the synthesis, and the newly constructed metal-halide layer consists of cesium cations in cubic coordination surrounded by four oxygens from the perovskite block and four chlorines from the new set of interlayer anions. Selected bond distances are given in Table 3. The Cs–O distances (3.191(6) Å) are comparable to those reported for eight-coordinate cesium in the $\text{CsLaNb}_2\text{O}_7$ parent compound (Cs–O: 3.191 Å),³⁴ and the Cs–Cl distances (3.496(1) Å) are similar to those of the CsCl salt itself (Cs–Cl: 3.57 Å).³⁵ Also, the metal-oxide distances in the perovskite block are quite consistent with published values.¹⁴ Rietveld refinement was also carried out on $(\text{Rb}_2\text{Cl})\text{LaNb}_2\text{O}_7$ (see Supporting Information); though the quality of the fit ($R_p = 9.71\%$,

(34) Kumada, N.; Kinomura, N.; Sleight, W. *Acta Crystallogr.* **1996**, C52, 1063.

(35) West, A. R. *Basic Solid State Chemistry*, 2nd ed.; John Wiley & Sons, LTD: New York, 1999.

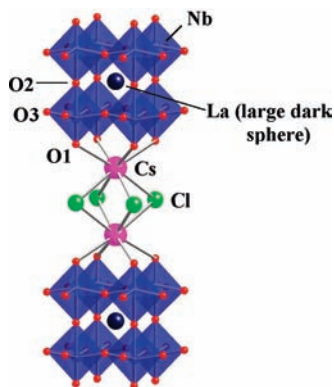


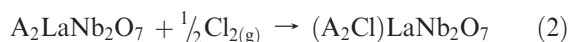
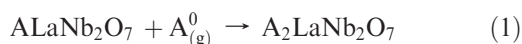
Figure 3. Structure of $(\text{Cs}_2\text{Cl})\text{LaNb}_2\text{O}_7$. Perovskite block contains NbO_6 polyhedra and lanthanum (large dark sphere).

$R_{\text{wp}} = 13.2\%$, and $\chi^2 = 3.5\%$) was not as good as with the cesium, the compound appears to be isostructural with $(\text{Cs}_2\text{Cl})\text{LaNb}_2\text{O}_7$.

Thermal analysis studies were carried out on $(\text{Rb}_2\text{Cl})\text{LaNb}_2\text{O}_7$ and $(\text{Cs}_2\text{Cl})\text{LaNb}_2\text{O}_7$. Both compounds decompose at elevated temperatures. HTXRD found that $(\text{Cs}_2\text{Cl})\text{LaNb}_2\text{O}_7$ starts to decompose slowly to $\text{CsLaNb}_2\text{O}_7$ and CsCl at $300\text{ }^\circ\text{C}$ with the decomposition complete by $800\text{ }^\circ\text{C}$. DSC showed no obvious transition on heating to $600\text{ }^\circ\text{C}$, consistent with a gradual decomposition; there is, however, an endotherm on heating at around $619\text{ }^\circ\text{C}$ and an exotherm on cooling around $607\text{ }^\circ\text{C}$ that is attributed to the melting and freezing of the decomposition byproduct, CsCl ($\text{mp} = 645\text{ }^\circ\text{C}$). Similar behavior is observed for $(\text{Rb}_2\text{Cl})\text{LaNb}_2\text{O}_7$ except that decomposition starts at slightly higher temperature, $400\text{ }^\circ\text{C}$, and is complete by $650\text{ }^\circ\text{C}$; DSC showed a similar endotherm on heating at $711\text{ }^\circ\text{C}$ and the exotherm on cooling at $702\text{ }^\circ\text{C}$ ($\text{mp}(\text{RbCl}) = 718\text{ }^\circ\text{C}$). Interestingly, HTXRD shows a much greater reduction in crystallinity for the decomposition products of the rubidium compound than of cesium.

Discussion

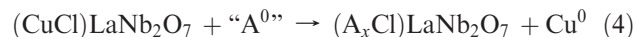
A two-step low temperature ($<400\text{ }^\circ\text{C}$) topochemical reaction strategy has been used to build alkali-metal-halide layers within a Dion–Jacobson-type double-layered perovskite. This method, which involves sequential reductive and oxidative intercalation steps (eqs 1 and 2),



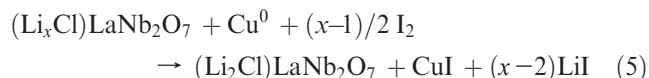
adds to the list of reactions effective in the construction of metal-anion layers within receptive hosts. While these reactions work well for building rubidium- and cesium-chloride layers, other reaction strategies have been reported for the formation of first-row transition-metal halide^{17–22} and alkali-metal chloride layers of lithium and sodium.^{25,26} In the fabrication of transition-metal-halide layers, for example, single-step ion-exchange reactions are effective (eq 3),



and in the case of the smaller alkali-metals ($A = \text{Li}, \text{Na}$), multistep reactions start with ion exchange (eq 3, $M = \text{Cu}$) to produce $(\text{CuCl})\text{LaNb}_2\text{O}_7$ from $\text{RbLaNb}_2\text{O}_7$, followed by reductive intercalation to form $(A_x\text{Cl})\text{LaNb}_2\text{O}_7$ ($A = \text{Li}, \text{Na}$; $2 \leq x < 4$) (eq 4). (Note that the copper metal byproduct can be removed by a subsequent treatment with iodine (eq 5).)



where " A^0 " = organo-lithium or sodium reagent,



These sets of reactions (eqs 1–5) are particular to the metal being targeted; divalent first-row transition-metal-halide layers can be made directly, while formation of the alkali-metal-halide layers utilizes multistep reactions. Access to a specific metal-halide layer is likely dependent on several factors including oxidation states, cation size, coordination preferences, and ion mobilities.

While the two-step intercalation approach presented here is effective for the formation of rubidium- and cesium-chloride layers, it did not prove successful in the formation of the corresponding lithium-, sodium-, and potassium-halide compounds. The lithium and sodium compounds are known (eq 4),^{25,26} so access to these phases is clearly dependent on the synthetic route. In the case of the smaller alkali metals it appears to be more effective to insert the halide ion in the interlayer prior to alkali-metal intercalation, while in the case of the larger alkali metals, the chloride can be inserted second. This is probably related in great part to the structures of the $A_2\text{LaNb}_2\text{O}_7$ intermediates. Structural details for both $\text{Li}_2\text{LaNb}_2\text{O}_7$ and $\text{Rb}_2\text{LaNb}_2\text{O}_7$ have been reported.^{13,14} Figure 4 highlights the interlayers for the two compounds. The lithium compound appears much less receptive to intercalation; its small interlayer spacing (9.31 \AA versus 11.14 \AA $\text{Rb}_2\text{LaNb}_2\text{O}_7$) combined with the cation "stuffed" interlayer, where the lithium cations reside in LiO_4 tetrahedra, likely suppresses the oxidative intercalation of the relatively large chloride ion. $\text{Rb}_2\text{LaNb}_2\text{O}_7$ by comparison has a much more open interlayer structure with the rubidium cations penetrating well into the hollows created by the four adjacent NbO_6 octahedra. This arrangement is expected to be more accommodating for the chloride ion in terms of both initial insertion and subsequent mobility during the nucleation and growth of the product phase.

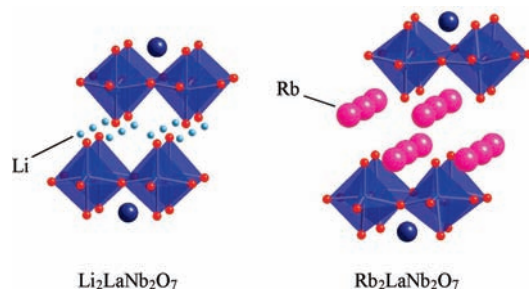


Figure 4. Comparison of the interlayer structures for the $\text{Li}_2\text{LaNb}_2\text{O}_7$ and $\text{Rb}_2\text{LaNb}_2\text{O}_7$ intermediates. Perovskite block contains NbO_6 polyhedra and lanthanum (dark blue sphere; structures from refs 13 and 14, respectively).

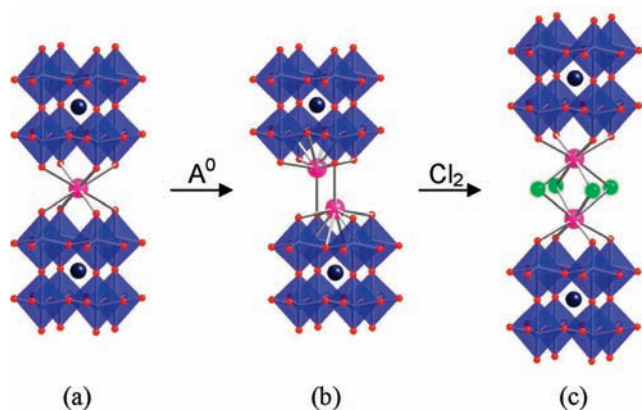


Figure 5. Structural transformation of (a) $\text{ALa Nb}_2\text{O}_7$ ($A = \text{Rb, Cs}$) to (b) $\text{A}_2\text{La Nb}_2\text{O}_7$ to (c) $(\text{A}_2\text{Cl})\text{La Nb}_2\text{O}_7$.

This synthetic approach allows the formation of alkali-halide layers with a CsCl -related structure. Here the coordinations of the rubidium and cesium cations are cubic with four oxygens from the perovskite layers and four chlorides from the newly constructed halide layer, AO_4Cl_4 ($A = \text{Rb, Cs}$). Cubic coordination is seen for both rubidium and cesium in the parent compounds, $\text{ALa Nb}_2\text{O}_7$.^{14,34} In terms of comparable halides, cubic coordination is not surprising for cesium in that it is what is observed for the simple CsCl salt; in contrast, the simple salt, RbCl , has the rock salt structure. In the previously reported lithium- and sodium-chloride double-layered perovskites, $(\text{A}_2\text{Cl})\text{La Nb}_2\text{O}_7$, the smaller relative size of these alkali metals results in tetrahedral coordination, AO_2Cl_2 ($A = \text{Li, Na}$).²⁵

The sequential intercalation of large alkali metals followed by chlorine into the Dion–Jacobson layered perovskites, $\text{ALa Nb}_2\text{O}_7$ ($A = \text{Rb, Cs}$), produces significant structural changes. Initially, the perovskite layers show an eclipsed orientation with the A cations in cubic coordination (Figure 5a).^{14,34} On reductive intercalation with alkali-metal, a major shift results such that the perovskite layers move to a staggered orientation (alternating layers shifted diagonally $1/2$ along a, b -plane); simultaneously, there is a doubling of the formal charge of the perovskite blocks with a corresponding increase in the alkali-metal cation content of the interlayer. Further, the A -cations move from the cubic site to a 9-coordinate site in the pocket of the perovskite layer, an arrangement common in Ruddlesden–Popper structural configurations (Figure 5b).¹⁴ Subsequently, on oxidative

intercalation of chlorine, the layer charge decreases and the cation attraction to the perovskite block lessens so that alkali-metal cations go back to cubic coordination (the cations become flanked by the perovskite layers on one side and the new chlorine layer on the other), as the layers revert to an eclipsed orientation (Figure 5c). Figure 5 highlights the structural variations observed in these processes.

Thermal analysis shows these compounds are low temperature phases, starting to decompose by $400\text{ }^\circ\text{C}$. Decomposition occurs with loss of the simple alkali-metal halide, ACl , and conversion of $(\text{A}_2\text{Cl})\text{La Nb}_2\text{O}_7$ back to the $\text{ALa Nb}_2\text{O}_7$ starting material; this loss of metal halide is similar to some of the transition-metal oxyhalides, $(\text{MCl})\text{La Nb}_2\text{O}_7$ ($M = \text{Fe, Cu}$), where decomposition occurs over a range of temperature with loss of the simple halide, MCl_2 , from $(\text{MCl})\text{La Nb}_2\text{O}_7$.²⁹ Information on the stability at elevated temperatures becomes important when considering efforts to further modify these compounds topochemically—subsequent manipulations will have to be carried out much below $400\text{ }^\circ\text{C}$, limiting the type of modifications that can be attempted.

In conclusion, a new two-step topochemical strategy for the construction of metal-halide layers within receptive hosts is presented. This method adds to the growing collection of reactions useful in building metal-anion arrays. The development of a comprehensive reaction library will serve to support rational syntheses targeting new compounds with potentially important magnetic, electronic, and structural properties. The two-step approach reported here is not expected to be limited, however, to the insertion of chloride anions. In fact, preliminary results indicate that other reagents beyond chlorine (e.g., oxygen, sulfur, and bromine) can also be used as intercalates.³⁶

Acknowledgment. This material is based upon work supported by the National Science Foundation under Grant 0612544.

Supporting Information Available: Listings of X-ray powder diffraction data and refined unit cells for all the parent compounds ($\text{ALa Nb}_2\text{O}_7$) and intermediates ($\text{A}_2\text{La Nb}_2\text{O}_7$), HTXRD data for both $(\text{Rb}_2\text{Cl})\text{La Nb}_2\text{O}_7$ and $(\text{Cs}_2\text{Cl})\text{La Nb}_2\text{O}_7$, and Rietveld refinement results for $(\text{Rb}_2\text{Cl})\text{La Nb}_2\text{O}_7$. This material is available free of charge via the Internet at <http://pubs.acs.org>.

(36) Choi, J.; Wiley, J. B., work in progress.